

## Preliminary Molecular Dynamics Simulation Studies of H-Y Zeolite in a Non-Rigid Zeolite Framework

Sang Gu Choi<sup>†</sup> and Song Hi Lee<sup>\*</sup>

*Department of Chemistry, Kyungsoong University, Pusan 608-736, Korea*

*<sup>†</sup>Department of Industrial Safety, Yangsan Junior College, Yangsan 626-800, Korea*

*Received December 7, 1998*

Molecular dynamics (MD) simulation of non-rigid H-Y zeolite framework are performed at 298.15 and 5.0 K. Usual bond stretching, bond angle bending, torsional rotational, and non-bonded Lennard-Jones and electrostatic interactions are considered as intraframework interaction potentials. Calculated atomic parameters are in good agreement with the experiment, which indicates the successful reproduction of the framework structure and its motion. Both calculated bond lengths and bond angles are also in good agreement with the experiment except generally for a little longer bond lengths and a little smaller T-O-H bond angles. The calculated overall site occupation of H<sup>+</sup> keeps the order O(2) > O(3) > O(4) > O(1) at 298.15 K, which is very different from the experimental prediction, O(1) > O(3) > O(2) at 5 K. Calculated IR spectra of the H-Y zeolite framework show that most of the main peaks of the O-H bonds are in the broad region 3700-5000 cm<sup>-1</sup> and that the O-T stretching bands appeared in 0-2000 cm<sup>-1</sup> and at 2700 cm<sup>-1</sup>

### Introduction

A number of structural studies have been reported to determine the cation positions in zeolites Y,<sup>1</sup> including some,<sup>1-8</sup> to locate the protons, which play a central role in acid catalysis. In the early studies, Olson and Dempsey<sup>2</sup> reported two hydrogen positions: one on a highly accessible bridging double 6-ring oxygen, O(1), and the other in the sodalite cavity near O(3). This report was partially supported by semiquantitative considerations of Mortier *et al.*<sup>3</sup> which indicate 17 protons per unit cell should bind to O(1), 10 to O(2), 28 to O(3), and 3 to O(4).

By using a new facility to determine the positions of hydrogen atoms in zeolites - neutron powder diffraction technique, Jirak *et al.*<sup>4</sup> found four different hydrogen positions in H-Y zeolites: those near O(1) and O(3) were highly occupied and those near O(2) and O(4) were nearly unoccupied. Czjzek *et al.*<sup>6</sup> studied D-Y zeolite containing water and completely dehydrated D-Y and H-Y zeolites, using high resolution neutron powder diffraction. The site occupation followed the order O(1) > O(3) > O(2) and no protons were located near O(4) in any of the three samples. The O-H bond lengths ranged from 0.83 to 1.17 Å.

Recently, Sun and Seff<sup>7,8</sup> reported the structure of Na-Y zeolite - largely ion exchanged with Pb<sup>2+</sup> at 100 °C and treated with D<sub>2</sub>S at 25 °C - based on pulsed-neutron powder diffraction methods. Two different positions are found for deuterium ions in the sample. Each of 18 deuterium ions in the large cavities bonds to an O(1) oxygen and lies in the plane of that oxygen and the two Si(Al) atoms to which O(1) is bound. In sodalite cavities, 16 deuterium ions bind similarly to O(3) oxygens.

The development of accurate, widely applicable, predictive methods for physico-chemical property estimation based on an understanding of the molecular-level processes is an enduring goal for physical chemists. Molecular dynam-

ics (MD) simulation methods play an increasingly important role in understanding the relationship between microscopic interactions and macroscopic physico-chemical properties. This is because MD simulation permits the researcher to selectively switch on and off key intermolecular interactions and evaluate their effect on the property of interest.

There have been a number of applications of MD simulation methods to zeolite-Y systems to investigate the local structure and dynamics of adsorbates in the zeolite-Y frameworks. For example, Yashonath *et al.* reported MD studies on time-dependent properties such as diffusion coefficients and intracrystalline site residence times for methane<sup>9</sup> and for benzene<sup>10</sup> in zeolite Y. They also reported adsorption properties of methane<sup>11</sup> and of xenon<sup>12</sup> in zeolite NaY. Schrimpf *et al.*<sup>13</sup> presented a force field for zeolite NaY, accounting for the flexibility of the lattice. They studied the flexibility of the inner void space at several temperatures by considering the diameter and the area of the windows connecting adjacent supercages. They also demonstrated the thermalization properties of the flexible framework with two examples, xenon and methane. Further studies of the group have focused on the diffusion of aromatic molecules in zeolite NaY by MD simulation.<sup>14-16</sup> Another computational study on the structure, vibrational properties and acidity in protonated H-Y zeolites was reported.<sup>17</sup>

Most of MD simulation studies, however, have concentrated on the dynamics of guest molecules in Na-Y zeolite systems, and dynamic and structural properties such as accurate determination of the positions of protons in H-Y zeolite by MD simulations have not been fully studied so far.

In our previous studies, we performed MD simulations of five rigid and three non-rigid zeolite-A systems to investigate the structure and dynamics of adsorbates: rigid dehydrated zeolite-A,<sup>18</sup> two rigid dehydrated Ca<sup>2+</sup>-exchanged zeolite-A systems,<sup>19</sup> rigid hydrated zeolite-A,<sup>20</sup> rigid dehydrated NH<sub>4</sub><sup>+</sup>-exchanged zeolite-A,<sup>21</sup> rigid dehydrated H<sup>+</sup>-

exchanged and  $\text{CH}_3\text{NH}_3^+$ -exchanged zeolite-A,<sup>22</sup> non-rigid zeolite-A framework-only system,<sup>23</sup> non-rigid dehydrated  $\text{H}^+$ -exchanged zeolite-A,<sup>24</sup> and non-rigid dehydrated zeolite-A.<sup>25</sup> The structure of the zeolite-A frameworks determined by the X-ray diffraction experiments<sup>26-31</sup> were used for these simulation studies.

Continuing our MD simulation studies of zeolite-A systems with rigid zeolite-A frameworks,<sup>18-25</sup> we present MD simulation of non-rigid zeolite-Y framework as the base case for a consistent study of the role of intraframework interaction on several zeolite-Y systems. The primary purpose of this work is to provide the basic non-rigid zeolite-Y framework, to test several intraframework interaction of zeolite Y, and to investigate the local structure and dynamics of adsorbates in the non-rigid zeolite-Y framework, especially the positions of protons in the H-Y zeolite.<sup>6</sup> In section II we present the molecular models and MD simulation method. We discuss our simulation results in section III and present the concluding remarks in section IV.

### Molecular Models and Molecular Dynamics Simulations

The structure of zeolite-Y framework is modeled by the unit cell,  $\text{Si}_{137}\text{Al}_{55}\text{O}_{384}$ , using the space group  $\text{Fd}\bar{3}\text{m}$  ( $a = 24.7665 \text{ \AA}$ ). The Si and Al atoms are assumed to be identical (denoted as T). The zeolite-Y framework is not assumed to be rigid, the framework atoms (T and O) are subject to move according to the equation of motion. The initial positions of the framework atoms are those determined by the neutron powder diffraction experiment of Czjzek *et al.*<sup>6</sup> for the H-Y zeolite system. In addition to the zeolite-Y framework atoms, the unit cell of the reported zeolite Y includes 53  $\text{H}^+$  and 3  $\text{Na}^+$  ions.

The structure of the modeled zeolite-Y framework is built up in principle by the corner-sharing of  $\text{TO}_4$  tetrahedra: a T atom is connected to four O atoms in a tetrahedral arrangement, and an O atom is connected to two T atoms, which gives a V-shape connection. The framework is composed of cubooctahedral sodalite cages linked together in a tetrahedral arrangement by six-membered rings (hexagonal prisms) of O(1) atoms to form large cavities (supercages). The supercages are interconnected in 4 ways by windows that are formed by rings consisting of 12 T and 12 O atoms (Figure 1<sup>32</sup>). One unit cell contains 8 sodalite cages, 16 hexagonal prisms, and 8 supercages.

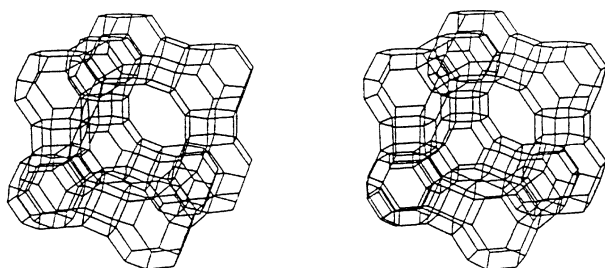


**Figure 1.** Structure of zeolite Y, the vertices of which are occupied by T atoms [32].

**Table 1.** Lennard-Jones parameters and electrostatic charges used in this study

atom	(nm)	(kJ/mol)	charge(e)
Al(=Si)	0.4009	0.5336	0.6666
O(1)	0.2890	0.6487	-0.3877
O(2)	0.2890	0.6487	-0.4155
O(3)	0.2890	0.6487	-0.4018
O(4)	0.2890	0.6487	-0.4137
$\text{H}^+$	0.0	0.0657	0.4895
$\text{Na}^+$	0.1776	20.8466	0.4895

The interaction potential for the framework atoms is given by the sum of bond stretching, bond angle bending, torsional rotational potential, and Lennard-Jones (LJ) and electrostatic non-bonded interactions. The usual LJ parameters and the electrostatic charges for the Coulomb potential are used in our previous studies,<sup>18-24</sup> and they are given in Table 1. Electrostatic charges of the framework atoms, for a given cation charge, were calculated by using Huheey's electronegativity set,<sup>33</sup> Sanderson's electronegativity equalization principle,<sup>34</sup> and the electric neutrality principle. In this work, we omit the Ewald summation<sup>35</sup> because of the long distance of a spherical cut-off of radius ( $12.38325 \text{ \AA}$ ), which is equal to half of the simulation box length.

In the unit cell of zeolite-Y framework,  $(\text{TO}_2)_{192}$ , 192 T atoms give a total of 768 T-O bonds. The T-O bond lengths of the  $\text{TO}_4$  tetrahedra differ according to the O atoms: T-O(1) = 0.16756, T-O(2) = 0.16326, T-O(3) = 0.16544 and T-O(4) = 0.16367 nm. The T-O bond stretching potential is given by a simple harmonic potential<sup>36</sup>

$$V(r) = \frac{k_r}{2}(r - r_{\text{eq}})^2$$

where  $k_r = 250,000 \text{ kJ/mol nm}^2$  and  $r_{\text{eq}}$  is used for each T-O bond length.

Since each  $\text{TO}_4$  tetrahedron gives 6 O-T-O angles, a total of 1152 O-T-O angles exists in the unit cell,  $(\text{TO}_2)_{192}$ . The O-T-O angles are O(1)-T-O(2) = 111.46, O(1)-T-O(3) = 107.07, O(1)-T-O(4) = 106.83, O(2)-T-O(3) = 108.73, O(2)-T-O(4) = 110.28, and O(3)-T-O(4) = 112.45 degrees. The O-T-O bond angle bending potential is also given by a simple harmonic potential

$$V(\theta) = \frac{k_\theta}{2}(\theta - \theta_{\text{eq}})^2$$

where  $k_\theta = 0.17605 \text{ kJ/mol-deg}^2$  and  $\theta_{\text{eq}}$  is used for each O-T-O angle.

Each O atom gives a T-O-T angle and a total of 384 T-O-T angles exists in the unit cell,  $(\text{TO}_2)_{192}$ . The T-O-T angles are T-O(1)-T = 135.61, T-O(2)-T = 144.55, T-O(3)-T = 139.75, and T-O(4)-T = 144.06 degrees. According to Nicholas *et al.*,<sup>36</sup> the T-O-T bond angle bending potential is given by an anharmonic potential

$$V(\theta) = \frac{k_{\theta 1}}{2}(\theta - \theta_{\text{eq}})^2 + \frac{k_{\theta 2}}{2}(\theta - \theta_{\text{eq}})^3 + \frac{k_{\theta 3}}{2}(\theta - \theta_{\text{eq}})^4 \quad (3)$$

where  $k_{\theta 1} = 0.013829$  kJ/mol-deg<sup>2</sup>,  $k_{\theta 2} = 0.00050542$  kJ/mol deg<sup>3</sup>,  $k_{\theta 3} = 0.000005148$  kJ/mol-deg<sup>4</sup> and  $\theta_{eq}$  is used for each T-O-T bond angle.

In silicates, the Si-O bond is known to lengthen as the Si-O-Si bond angle becomes smaller.<sup>37</sup> The exact relationship between the bond length and bond angle depends on the compound and also varies with the amount of Al in the lattice. To reproduce the correct dynamic behavior of the lattice, the Urey-Bradley term is needed, based on the T-T non-bonded distance for each T-O-T angle

$$V(r) = \frac{k_r}{2}(r - r_{eq})^2 \quad (4)$$

where  $k_r = 22,845$  kJ/mol-nm<sup>2</sup> and  $r_{eq}$  is used for each T-T distance - 0.31029, 0.31102, 0.31067, and 0.31137 nm.

In a dihedral angle, which is associated with four consecutive atoms(O-T\*-O\*-T), a torsional rotational potential on the T\*-O\* bond is possible since the three O atoms connected to T\*, except the O\* atom, are restricted by the O-T\*-O angle bending potentials. In the unit cell, (TO<sub>2</sub>)<sub>192</sub>, there are 384 T-O-T angles. Since we can pick up one among three O atoms connected to each T atom to make a dihedral angle, there can be a total of 768 dihedral angles. The torsional rotational potential for the O-T-O-T dihedral angle is a periodic function with a 3-fold barrier:

$$V(\phi) = \frac{k_{\phi}}{2}[1 + \cos(3\phi)] \quad (5)$$

where  $k_{\phi} = -2.9289$  kJ/mol.

A canonical ensemble of fixed N (number of particles), V (volume of fixed zeolite framework), and T (temperature) is chosen for the simulation ensemble. Gauss's principle of least constraint<sup>38</sup> is used to maintain the system at the constant temperatures of 5.0 K and 298.15 K. The ordinary periodic boundary condition in the x-, y-, and z-direction and minimum image convention are applied for the Lennard-Jones potential with a spherical cut-off of radius equal to half of each simulation box length. Gear's fifth order predictor-corrector method<sup>39</sup> is used to solve the equations of translational motion of the framework atoms with a time step of  $1.0 \times 10^{-16}$  sec. The equilibrium properties are averaged over five blocks of 100,000 time steps for a total of 500,000 time steps after 500,000 time steps to reach an equilibrium state. The configuration of each ion is stored every 4 time steps for further analysis.

## Results and Discussion

The neutron powder diffraction study for the H-Y zeolite (H<sub>53</sub>Na<sub>3</sub>Si<sub>136</sub>Al<sub>56</sub>O<sub>384</sub>) shows that the site occupancies of H<sup>+</sup> follow the order O(1) > O(3) > O(2) > O(4) with occupancies of 28.6, 9.5, 15.0, and 0.0, and for Na<sup>+</sup>, 3 occupancies on the site I with none on the sites I' and II.<sup>6</sup> The occupation of H<sup>+</sup> is idealized by 28, 10, and 15 for H(1), H(2), and H(3), respectively, for simplicity in this study. The 53 H<sup>+</sup> and 3 Na<sup>+</sup> ions are distributed within the unit cell on the 16 hexagonal prisms in order to minimize the distance between those

**Table 2.** Distribution of 53 H<sup>+</sup> and 3 Na<sup>+</sup> ions at 16 hexagonal prisms as the initial positions

hexagonal prism	H(1)	H(2)	H(3)	Na+	total
1	1	1	0	1	3
2	2	1	1	0	4
3	2	0	2	0	4
4	2	0	1	0	3
5	2	1	1	0	4
6	2	0	2	0	4
7	2	0	1	0	3
8	1	1	0	1	3
9	2	0	1	0	3
10	2	0	1	0	3
11	2	1	1	0	4
12	2	1	1	0	4
13	1	1	0	1	3
14	2	1	1	0	4
15	2	1	1	0	4
16	1	1	1	0	3
total	28	10	15	3	56

ions, and the final positions are listed in Table 2. In each hexagonal prism, 6 equipositions for H(1), 6 for H(2), 6 for H(3), and 6 for H(4) exist. The positions of these equipositions for H<sup>+</sup> are given in the experimental and calculated refined atomic parameters (see Table 3).

Three different MD simulations for the H-Y zeolite (H<sub>53</sub>Na<sub>3</sub>Si<sub>136</sub>Al<sub>56</sub>O<sub>384</sub>)<sup>6</sup> system were carried out. The first system is initially fixed at 298.15 K, the second one is cooled down to 5.0 K from the first one at 298.15 K (referred as 5.0 K(A)), and the third one is initially at 5.0 K (referred as 5.0 K(B)). It is worth noting that the choice of a Lennard-Jones parameter,  $\sigma$ , for H<sup>+</sup> ion is somewhat tangled. The values of  $\sigma$  for H<sup>+</sup> ion used in the study of H<sub>12</sub>-A zeolite using non-rigid dehydrated zeolite-A framework<sup>24</sup> are too large to give a proper O-H distance in this study. The final value for  $\sigma$  for H<sup>+</sup> ion is chosen as zero without any change of  $\sigma$  for the framework atoms, especially O atoms.

In Table 3, the results of the experimental and calculated structural parameters of zeolite Y are compared. The mean crystallographic positions and the mean-square displacement matrices **B** are obtained by referring the values of the individual atoms back to the asymmetric unit by symmetry operations.<sup>40</sup> The elements of the symmetric 3×3 matrix **B** are computed as  $u_{ij} = \langle u_i u_j \rangle = \langle r_i r_j \rangle - \langle r_i \rangle \langle r_j \rangle$  and then the values of the isotropic B factors are obtained as  $B_{iso} = 8/3 \pi^2$  trace (**B**). These values calculated from our MD simulations are generally lower due to the fact that long-wave phonons are not reproduced with systems of unit cell dimensions.<sup>41</sup> It is known that these phonons make a considerable contribution to the thermal motion of the atoms. The small values of  $B_{iso}$  for Na<sup>+</sup> ions at 5.0 K (B) are notable. The agreement between the experimental and calculated coordinates is generally quite good with the mean deviations of 0.025 Å, 0.025 Å, and 0.022 Å at 298.15, 5.0 (A), and 5.0 K (B) for the framework atoms and with those of 0.229 Å, 0.300 Å, and

**Table 3.** Experimental [5] and calculated refined atomic parameters ( $a = 24.7665 \text{ \AA}$ )

atom, position	x/a	y/a	z/a	$B_{\text{iso}}$	N
Si(Al), 192i					
exp.	-0.0526	0.0362	0.1249	1.033	192
298.15 K	-0.0531	0.0359	0.1254	0.672	192
5.0 K (A)	-0.0531	0.0359	0.1254	0.641	192
5.0 K (B)	-0.0529	0.0360	0.1255	0.222	192
O(1), 96h					
exp.	0.0	-0.10682	0.10682	1.481	96
298.15 K	-0.00006	-0.10689	0.10684	0.694	96
5.0 K (A)	0.00007	-0.10692	0.10684	0.653	96
5.0 K (B)	-0.00004	-0.10689	0.10690	0.543	96
O(2), 96g					
exp.	-0.0027	-0.0027	0.1434	2.416	96
298.15 K	-0.0031	-0.0033	0.1419	1.125	96
5.0 K (A)	-0.0031	-0.0034	0.1418	1.124	96
5.0 K (B)	-0.0032	-0.0033	0.1424	0.597	96
O(3), 96g					
exp.	0.1787	0.1787	-0.0337	2.368	96
298.15 K	0.1774	0.1774	-0.0337	0.697	96
5.0 K (A)	0.1774	0.1774	-0.0336	0.663	96
5.0 K (B)	0.1775	0.1775	-0.0331	0.239	96
O(4), 96g					
exp.	0.1751	0.1751	0.3213	1.809	96
298.15 K	0.1770	0.1770	0.3204	0.701	96
5.0 K (A)	0.1771	0.1771	0.3205	0.667	96
5.0 K (B)	0.1768	0.1768	0.3207	0.081	96
Na, 16c					
exp.	0.0	0.0	0.0	7.0	3.0
298.15 K	0.0073	0.0072	0.0072	0.119	3.0
5.0 K (A)	0.0052	0.0051	0.0051	0.134	3.0
5.0 K (B)	0.0049	0.0048	0.0046	0.029	3.0
H(1), 96h					
exp.	0.0	-0.1304	0.1304	3.4	28.61
298.15 K	0.0163	-0.1372	0.1388	0.351	9.66
5.0 K (A)	0.0127	-0.1364	0.1400	0.339	10.00
5.0 K (B)	0.0145	-0.1369	0.1389	0.338	28.00
H(2), 96g					
exp.	0.007	0.007	0.182	3.4	9.52
298.15 K	0.0179	0.0213	0.1760	0.310	16.66
5.0 K (A)	0.0231	0.0302	0.1601	0.268	15.00
5.0 K (B)	0.0121	0.0139	0.1825	0.257	10.00
H(3), 96g					
exp.	0.1909	0.1909	0.002	3.4	15.04
298.15 K	0.1967	0.2004	0.0031	0.356	14.64
5.0 K (A)	0.1991	0.1981	0.0019	0.345	15.00
5.0 K (B)	0.1898	0.1912	0.0098	0.249	15.00
H(4),					
exp.	-	-	-	-	-
298.15 K	0.2009	0.2020	0.3520	0.352	12.04
5.0 K (A)	0.1992	0.2001	0.3537	0.285	13.00
5.0 K (B)	-	-	-	-	0.00

0.164  $\text{\AA}$  at 298.15 K, 5.0 K (A), and 5.0 K (B) for the cations. These values of the mean deviations are comparable

**Table 4.** Average potential energies (kJ/mol) of framework atoms and cations for 500,000 time steps (50 ps)

atom or cations	energy		
	298.15 K	5.0 K (A)	5.0 K (B)
Na(1)	-179.5	-171.8	-165.3
Na(2)	-208.6	-179.0	-45.2
Na(3)	-179.2	-254.5	-78.8
H(1)	-208.9	-251.7	-261.8
H(2)	-178.5	-200.7	-158.2
H(3)	-148.0	-136.5	-212.6
H(4)	-190.9	-133.4	-
O(1)	309.7	291.2	264.9
O(2)	247.6	321.1	318.2
O(3)	246.6	323.9	317.7
O(4)	319.1	249.1	252.3
T	630.8	585.7	578.0

with those of Demontis *et al.*<sup>42</sup> for non-rigid dehydrated zeolite-A system and those of Schrimpf *et al.*<sup>13</sup> for non-rigid zeolite NaY, and are much better than those in the study of non-rigid zeolite-A framework only,<sup>23</sup> probably due to the use of the individual bond distances and bond angles for the bond stretching and bond angle bending potentials in this study instead of the use of the averages in that study.

The occupation of H(1), H(2), H(3), and H(4) predicted by the neutron powder diffraction study for the H-Y zeolite ( $\text{H}_{53}\text{Na}_3\text{Si}_{136}\text{Al}_{56}\text{O}_{384}$ ) at 5 K<sup>6</sup> is 28.6, 9.5, 15.0, and 0.0, respectively, but these values are initially idealized by 28, 10, 15, and 0 for our MD simulations in this study as discussed at the beginning of this section. The positions of  $\text{H}^+$  and  $\text{Na}^+$  ions are never changed in the entire run of our MD simulation at 5.0 K (B). The stability order of  $\text{O}(1) > \text{O}(3) > \text{O}(2)$  is well explained by the average potential energies of  $\text{H}^+$  ions and framework O atoms in Table 4. At 298.15 K, however, the movement of  $\text{H}^+$  ions is more vigorous: the respective average occupation of H(1), H(2), H(3), and H(4) is 9.66, 16.66, 14.64, and 12.04 and hence the overall site occupation of  $\text{H}^+$  keeps the order  $\text{O}(2) > \text{O}(3) > \text{O}(4) > \text{O}(1)$  at 298.15 K. The appearance of new occupation of  $\text{H}^+$  ions at O(4) is notable. The occupation of  $\text{H}^+$  ions at O(4) was reported by semiquantitative considerations of Mortier *et al.*<sup>3</sup> This result from our MD simulation at 298 K is very different from the experimental prediction,<sup>6</sup>  $\text{O}(1) > \text{O}(3) > \text{O}(2)$  at 5 K and also different from the pulsed-neutron powder diffraction experimental prediction for sodium zeolite Y by Sun and Seff<sup>7,8</sup> which reported 18.0 deuterium ions per unit cell bound to O(1) and 16.1 to O(3). The average potential energies of  $\text{H}^+$  ions and framework O atoms at 298.15 K in Table 4 offer a rather subtle explanation for the order of the overall site occupation of  $\text{H}^+$  ions. The system at 298.15 K is gradually cooled down to 5.0 K and is equilibrated for 500,000 time steps. The positions of  $\text{H}^+$  and  $\text{Na}^+$  ions are never changed in the next 500,000 time steps for averaging at 5.0 K (A) and the occupation of H(1), H(2), H(3), and H(4) is nearly frozen from those at 298.15 K.

**Table 5.** Experimental[6] and calculated bond lengths (Å) and bond angles (deg) of protons to the framework atoms

lengths and angles	exp.	cal.		
		298.15 K	5 K (A)	5 K (B)
T-H(1)	2.132(8)	2.164(4)	2.172(6)	2.173(4)
T-H(2)	2.19(3)	2.19(11)	2.08(10)	2.21(10)
T-H(3)	2.17(4)	2.29(9)	2.30(8)	2.35(8)
T-H(4)	-	2.58(7)	2.50(9)	-
O(1)-H(1)	0.83(2)	1.17(6)	1.14(9)	1.15(7)
O(2)-H(2)	1.02(5)	1.16(9)	1.15(11)	1.15(10)
O(3)-H(3)	0.98(4)	1.18(9)	1.15(7)	1.16(6)
O(4)-H(4)	-	1.16(8)	1.14(6)	-
T-O(1)-H(1)	112.2(8)	98.1(8)	99.6(8)	99.2(9)
T-O(2)-H(2)	107.6(10)	102.3(10)	95.5(10)	104.6(11)
T-O(3)-H(3)	109.8(8)	106.2(8)	108.5(6)	111.0(6)
T-O(4)-H(4)	-	128.6(9)	129.2(9)	-

In Table 5, we compared the experimental and calculated bond lengths and bond angles of protons to the framework atoms. The overall agreement is quite good except for the T-O(1)-H(1) and T-O(2)-H(2) angles. The increment of the O-H bond lengths and the small change of the T-H bond lengths without change of the T-O bond lengths makes the T-O-H angles smaller compared with the experimental case. The order of the experimental O-H bond lengths reflects the site occupation of H<sup>+</sup> with the order as O(1) > O(3) > O(2) very well. The variation of the calculated O-H bond lengths from our MD simulations is almost the same for all the O-H bonds and makes it impossible to predict the site occupation of H<sup>+</sup> ion at the framework O atoms. One notes that the O-H bond lengths decrease with decreasing temperature but not the T-H bond lengths. The O(4)-H(4) bond length is comparable with the other O-H bond lengths, but the T-H(4) bond length is much longer than the other T-H bond lengths and that makes the T-O(4)-H(4) bond angle larger than the others.

The IR spectra of zeolite systems are calculated by Fourier transformation of the dipole moment autocorrelation function.<sup>43</sup> Figure 2 shows the calculated IR spectra of zeolite-Y framework from the dipole moment autocorrelation functions of each O-H bonds and the total O-T bonds at 298.15 K. First, most of the main peaks of the O-H bonds are in the broad region 3700-5000 cm<sup>-1</sup>, which is attributed to O-H stretching. For comparison, the broad peaks are averaged to give the most probable frequency. The calculated average frequencies are 4420 cm<sup>-1</sup> for O(1)-H(1), 4430 cm<sup>-1</sup> for O(2)-H(2), 4160 cm<sup>-1</sup> for O(3)-H(3), and 4590 cm<sup>-1</sup> for O(4)-H(4). These values are somewhat higher than the two experimental O-H stretching bands in the IR spectrum of zeolite Y - 3650 cm<sup>-1</sup> for O(1)-H(1) and 3550 cm<sup>-1</sup> for O(3)-H(3), which are the active sites in acidic catalysis.<sup>44-48</sup> It is possible to obtain accurate bands of the IR spectrum from MD simulations of zeolite Y by using refined Lennard-Jones parameters for the framework atoms and cations and refined bond stretching and bond angle bending potentials for the zeolite-Y framework. Second, the O-T stretching bands

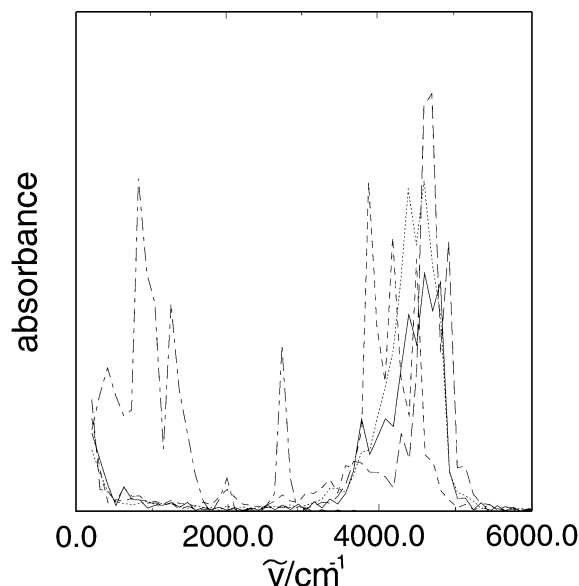


**Figure 2.** IR spectra of zeolite Y at 298.15 K, calculated from the O(1)-H(1) dipole moment autocorrelation function (—), the O(2)-H(2) (·····), the O(3)-H(3) (-----), the O(4)-H(4) (- - - -), and the total dipole moment autocorrelation function of zeolite-Y framework (-----).

appeared in 0 2000 cm<sup>-1</sup> and at 2700 cm<sup>-1</sup>. The spectra are much different from that of non-rigid zeolite-A framework only system,<sup>23</sup> which has a large peak at 2700 cm<sup>-1</sup> from the simple harmonic oscillation of the total dipole moment autocorrelation function, reflecting a monotonous dynamical feature of the framework.

Although this preliminary study demonstrates the usefulness of the approach presented and therefore justifies further uses of the same methodology, we should note that several points should be reconsidered in a further study. First, Si-O-Al moieties: Si and Al are treated as identical in this model, but it is doubtful that the observed binding preferences of protons to the four crystallographically distinct oxygens in the zeolite Y are accurately reproduced. Second, the long-range electrostatics is ignored. Since any long-range forces are non-negligible for any finite cut-off distance, not performing the Ewald summation<sup>34</sup> may contribute additional errors to the observed proton binding preferences. Third, the nature of the proton-framework interaction is not specified as a harmonic valence bond form. If that is the case, proton redistribution should be impossible, since the harmonic potentials should go to infinity during a proton jump. But it is possible to use switching functions that turn harmonic forces on and off depending upon distance.

## Conclusion

A molecular dynamics simulation of non-rigid H-Y zeolite framework was performed at 298.15 K and 5.0 K. Calculated atomic parameters, bond lengths, and bond angles are in good agreement with the experimental, which indicates the successful reproduction of the framework structure and its motion. The calculated overall site occupation of H<sup>+</sup>

keeps the order  $O(2) > O(3) > O(4) > O(1)$  at 298.15 K. The IR spectra of H-Y zeolite system calculated by Fourier transformation of the dipole moment autocorrelation function show most of the main peaks of the O-H bonds are in the broad region 3700-5000  $\text{cm}^{-1}$  with calculated average frequencies of 4420  $\text{cm}^{-1}$  for O(1)-H(1), 4430  $\text{cm}^{-1}$  for O(2)-H(2), 4160  $\text{cm}^{-1}$  for O(3)-H(3), and 4590  $\text{cm}^{-1}$  for O(4)-H(4). The O-T stretching bands appeared in 0-2000  $\text{cm}^{-1}$  and at 2700  $\text{cm}^{-1}$ .

**Acknowledgment.** This work was supported in part by a research grant to SGC from the Korea Research Foundation, 1996, and in part by a research grant to SHL from Kyung-sung University (research fund for basic data), 1996. The authors would like to thank the Computer Center at Korea Institute of Science and Technology for access to the Cray-C90 system and the Tongmyung University of Information Technology for access to its IBM SP/2 computers.

### References

- Mortier, W. J. *Compilation of Extra-Framework Sites in Zeolites*; Butterworth: Guildford, UK, 1982.
- Olson, D. H.; Dempsey, E. J. *Catal.* **1969**, *13*, 221.
- Mortier, W. J.; Pluth, J. J.; Smith, J. V. *J. Catal.* **1976**, *45*, 367.
- Jirak, Z.; Vratislav, S.; Bosacek, V. *J. Phys. Chem. Solids* **1980**, *41*, 1089.
- Cheetham, A. K.; Eddy, M. M.; Thomas, J. M. *J. Chem. Soc., Chem. Commun.* **1984**, 1337.
- Czjzek, M.; Jobic, H.; Fitch, A. N.; Vogt, T. *J. Phys. Chem.* **1992**, *96*, 1535.
- Sun, T.; Seff, K. *J. Catal.* **1992**, *138*, 405.
- Sun, T.; Seff, K. *J. Phys. Chem.* **1993**, *97*, 7719.
- Yashonath, S.; Demontis, P.; Klein, M. L. *Chem. Phys. Lett.* **1988**, *153*, 551.
- Demontis, P.; Yashonath, S.; Klein, M. L. *J. Phys. Chem.* **1989**, *93*, 5016.
- Yashonath, S.; Demontis, P.; Klein, M. L. *J. Phys. Chem.* **1991**, *95*, 5881.
- Yashonath, S. *Chem. Phys. Lett.* **1991**, *177*, 54.
- Schrimpf, G.; Schlenkrich, M.; Brickmann, J.; Bopp, P. *J. Phys. Chem.* **1992**, *96*, 7404.
- Klein, H.; Fuess, H.; Schrimpf, G. *J. Phys. Chem.* **1996**, *100*, 11101.
- Mosell, T.; Schrimpf, G.; Brickmann, J. *J. Phys. Chem. B* **1997**, *101*, 9476.
- Mosell, T.; Schrimpf, G.; Brickmann, J. *J. Phys. Chem. B* **1997**, *101*, 9485.
- Schroder, K.-P.; Sauer, J.; Leslie, M.; Catlow, C. R. A.; Thomas, J. M. *Chem. Phys. Lett.* **1992**, *188*, 320.
- Moon, G. K.; Choi, S. G.; Kim, H. S.; Lee, S. H. *Bull. Korean Chem. Soc.* **1992**, *13*, 317.
- Moon, G. K.; Choi, S. G.; Kim, H. S.; Lee, S. H. *Bull. Korean Chem. Soc.* **1993**, *14*, 356.
- Lee, S. H.; Moon, G. K.; Choi, S. G.; Kim, H. S. *J. Phys. Chem.* **1994**, *98*, 1561.
- Choi, S. G.; Lee, S. H. *Mol. Sim.* **1996**, *17*, 113. In Figs. 2, 3, 4, and 5, NH4(2) and NH4(3) should be replaced by each other.
- Lee, S. H.; Choi, S. G. *J. Phys. Chem. B* **1997**, *101*, 8402.
- Lee, S. H.; Choi, S. G. *Bull. Korean Chem. Soc.* **1998**, *19*, 422.
- Lee, S. H.; Choi, S. G. *Bull. Korean Chem. Soc.* in press.
- Lee, S. H.; Choi, S. G. submitted in *Bull. Korean Chem. Soc.*
- Pluth, J. J.; Smith, J. V. *J. Am. Chem. Soc.* **1980**, *102*, 4704.
- Pluth, J. J.; Smith, J. V. *J. Am. Chem. Soc.* **1983**, *105*, 1192.
- Jang, S. B.; Han, Y. W.; Kim, D. S.; Kim, Y. *Kor. J. Crystal.* **1990**, *1*, 76.
- Seff, K.; Shoemaker, D. P. *Acta Crystallogr.* **1967**, *22*, 162.
- Gramlich, V.; Meier, W. M. *Z. Kristallogr.* **1971**, *133*, 134.
- McCusker, L. B.; Seff, K. *J. Am. Chem. Soc.* **1981**, *103*, 3441.
- Meier, W. M.; Olson, D. H.; Baerlocher, Ch. *Zeolites* **1996**, *17*, 1.
- Huheey, E. *J. Phys. Chem.* **1965**, *69*, 3284.
- Sanderson, R. T. *Chemical Periodicity*; Reinhold: New York, 1960.
- (a) de Leeuw, S. W.; Perram, J. W.; Smith, E. R. *Proc. R. Soc. London* **1980**, *A373*, 27. (b) Anastasiou, N.; Fincham, D. *Comput. Phys. Commun.* **1982**, *25*, 159.
- Nicholas, J. B.; Hopfinger, A. J.; Trouw, F. R.; Iton, L. X. *J. Am. Chem. Soc.* **1991**, *113*, 4792.
- Genechten, K. A. V.; Mortier, W. J. *Zeolites* **1988**, *8*, 273.
- Gauss, K. F. *J. Reine. Angew. Math.* **1829**, *IV*, 232.
- Gear, C. W. *Numerical initial value problems in ordinary differential equation*; Englewood Cliffs NJ: Prentice-Hall, 1971.
- Willis, B. T. M.; Pryor, A. W. *Thermal Vibrations in Crystallography*; Cambridge University Press; Cambridge, 1975.
- Black, J. E.; Bopp, P. *Surf. Sci.* **1987**, *182*, 98.
- Demontis, P.; Suffritti, G. B.; Quartieri, S.; Fois, E. S.; Gamba, A. *J. Phys. Chem.* **1998**, *92*, 867.
- Behrens, P. H.; Wilson, K. R. *J. Chem. Phys.* **1981**, *74*, 4872.
- Ward, J. W. *J. Catal.* **1967**, *9*, 225.
- Ward, J. W. *J. Catal.* **1968**, *10*, 34.
- Uytterhoeven, J. B.; Jacobs, P.; Makay, K.; Schoonheydt, R. *J. Phys. Chem.* **1968**, *72*, 1768.
- Ward, J. W.; Hansford, R. C. *J. Catal.* **1969**, *13*, 364.
- Ward, J. W. In *Zeolite Chemistry and Catalysis*; Rabo, J. A., Ed.; ACS Symposium Series; American Chemical Society; Washington, DC, 1976.; Vol. 171, p 118.